ACS OMEGA

Open Access

http://pubs.acs.org/journal/acsodf

Article

Experimental and Molecular Dynamics Simulation to Investigate Oil Adsorption and Detachment from Sandstone/Quartz Surface by Low-Salinity Surfactant Brines

Ernest Peter Maiki, Renyuan Sun,* Shaoran Ren, and Ayman Mutahar AlRassas

Cite This: *ACS Omega* 2024, 9, 20277−20292

Read Online

ACCESS | Metrics & More | Article Recommendations

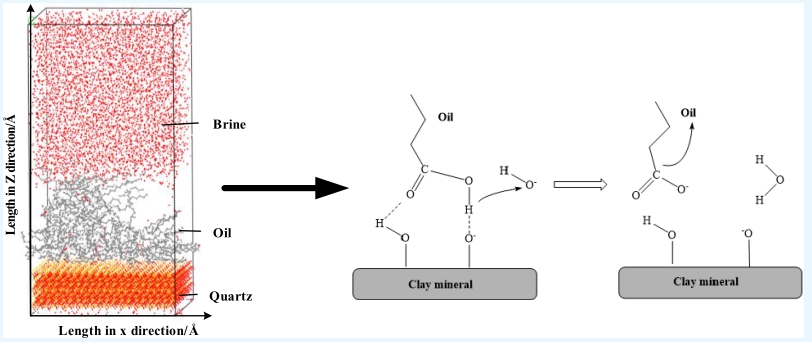

ABSTRACT: In this study, we explore the impact of monovalent (NaCl) and divalent ($CaCl_2$) brines, coupled with sodium dodecyl sulfate (SDS) surfactant at varying low concentrations, on the detachment and displacement of oil from sandstone rock surfaces. Employing the sessile drop method and molecular dynamics simulations, we scrutinize the behavior of the brine solutions. Our findings reveal that both low salinity and low-salinity surfactant solutions induce a gradual shift in rock wettability toward a more water-wet state. This wettability transformation is not instantaneous but evolves over time, as observed through meticulous molecular motion analyses. Through contact angle measurements and molecular dynamics simulations, we delve into the molecular motion at subpore and micropore scales on sandstone/quartz surfaces. The adsorption of surface-active agents from the oil to the oil−brine interface results in a reduced interfacial tension, significantly contributing to oil displacement. Notably, low salinity concentrations ranging from 1000 to 10,000 ppm exhibit the lowest contact angles within 30 min across all solutions. However, higher concentrations deviate from this declining trend, especially with divalent ions like Ca^{2+}, which bridge polar molecules onto the rock surface, resulting in an increased oil-wetting state. This research unveils the intricate molecular motions involved in employing low-salinity surfactant solutions for oil detachment from surfaces. Furthermore, it provides valuable insights into the underlying forces driving oil detachment and wettability alteration.

1. INTRODUCTION

Since George G. Bernard introduced low-salinity water flooding (LSW) in 1967, it has been considered a promising method to enhance oil recovery.[1] This approach has become one of the most extensively studied areas, aiming to uncover the underlying mechanisms and determine the optimal brine composition.[2,3] The effectiveness of low-salinity water flooding is highly contingent on the characteristics of the crude oil−brine-rock (COBR) system.[4−7] Indeed, low-salinity water flooding stands out as an economical method for enhanced oil recovery (EOR), notable for its avoidance of toxic and costly materials. In recent times, there has been an increased emphasis on low-salinity water research and its synergy with other fluids such as surfactants, polymers, and so forth.[8−11] The primary goal is to minimize brine−oil interfacial tension, enhancing the efficacy of the recovery process. This approach has demonstrated superior outcomes when contrasted with high brine concentrations, supported by robust field data and academic research.[8,11−15] These studies have prominently focused on documenting wettability alteration in oil reservoirs, acknowledging its crucial role in attaining successful oil recovery. The phenomenon under scrutiny, commonly denoted as the low salinity effect (LSE), entails the unmistakable modification of rock surface wettability.[16−18] This alteration plays a vital role in improving the detachment and flow of oil.

Received: January 22, 2024
Revised: March 27, 2024
Accepted: April 4, 2024
Published: April 22, 2024

Bai et al. studied model asphaltene molecules with varied heteroatoms strategically placed. Their investigation centered on the application of molecular dynamic simulation techniques to delve into and analyze the adsorption and desorption behaviors of asphaltene molecules.[19] They observed asphaltene molecule detachment intricately influenced by the interplay between asphaltene−silica and asphaltene−water interactions. Furthermore, the heteroatom type and arrangement in space were recognized for enhancing interactions between asphaltene and silica. Notably, sulfur (S) atoms were found to strengthen van der Waals interactions, thereby impeding the detachment of asphaltene from the surface. This emphasizes the nuanced role of heteroatoms, particularly sulfur, in regulating the dynamic interactions between asphaltene molecules and silica surfaces during desorption processes.[19] Lager et al. suggested a mechanism wherein polar organic oil molecules form bonds with the rock surface through bridging by divalent ions.[20] Upon the injection of low-salinity brine, monovalent ions easily exchanged with the bridging ions, following a multicomponent ion exchange (MIE) process, ultimately releasing the oil.[21−23] This migration of divalent ions aligns with the forecasts of the DLVO theory, indicating that the addition of a low-salinity solution triggers the expansion of the electric double layer (EDL). This EDL expansion serves as the foundation for several other low salinity effect (LSE) hypotheses.[24−26] Hosseinzade et al. observed that an increase in ionic strength, characterized by the divalent ion/Na^+ ratio ranging from 0 to 0.033, resulted in conflicting impacts. This led to a reduction in interfacial tension (IFT), promoting enhanced oil recovery, while there was an increase in surfactant adsorption, thereby diminishing the potential for EOR. The predominance of the ionic strength effect was evident at the 0.0175 Ca^{2+}/Na^+ ratio. In essence, while water-wetness and/or oil recovery commonly decline with higher $CaCl_2$ concentrations, a detailed atomistic-level understanding is crucial in this context.[23] Yue et al. observed that oil film detachment from the sandstone surface was contingent upon overcoming disjoining pressure. The results highlighted the interplay of both repulsive and attractive forces. The repulsion arose from the charges or ions at the interfaces of brine/oil and brine/rock, preventing the oil from reaching the rock surface and inhibiting the wetting process.[27]

These findings account for the crucial milestones in unraveling the intricate interaction dynamics between crude oil and brine, as well as the impact of reservoir lithology on tertiary oil extraction.[28] The correlation between fluid−fluid and fluid−rock interactions and their influence on interfacial tension (IFT) is paramount, as emphasized in this article through contact angle measurements and molecular dynamics simulations. Additionally, the study delves into the roles of brine ions and sodium dodecyl sulfate (SDS) surfactants at the oil−brine interface, underscoring their critical contributions to oil displacement. Molecular dynamics (MD) simulations provide valuable insights into the atomistic interaction paradigm at both the subpore and pore levels.[29,30] These ionic contributions at the oil−brine and rock interfaces, studied at multiple scales, serve as a foundation for evaluating the role of brine ions and their contribution to the removal of adsorbed crude oil and displacement from rock surfaces.[31−34] MD simulations provide a better understanding of the atomistic interactions occurring at various scales, while the influence of low salinity on oil−brine interfaces and wettability alteration is investigated through contact angle measurements and molecular dynamics analysis.[35−37]

These simulations offer valuable insights that contribute to the refinement of existing models for fluid flow on surfaces and the associated intermolecular interactions. Moreover, molecular dynamics facilitates the observation and microscopic detection of the liquid wetting behavior on rock surfaces. This capability enables a detailed analysis of the characteristic behavior through molecular dynamics analysis, thereby advancing our comprehension of these complex systems.[35,38,39] Underwood and Greenwell investigated the salinity dependence of interfacial tension (IFT) for decanes in contact with aqueous NaCl solutions. They observed a decrease in boundary layer thickness with increasing brine salinity, resulting in higher IFTs.[40] This phenomenon needs to be explained in terms of molecular motion. Zhao et al. expanded on related work by focusing on diluted NaCl solutions and observed a nonmonotonic trend in IFT for *n*-decane/brine systems, which contributes to improved oil recovery.[41] Remesal et al. investigated the effect of monovalent and divalent brines (NaCl and $CaCl_2$) on oil dodecane and benzene and found that calcium ions were more surface-active than sodium ions due to their larger hydration shell.[42]

Understanding the behavior of polar compounds in crude oil and their interaction with brine cations at the interface is crucial for comprehending the effect of salinity on oil−brine interfaces, which is a focus of this study. The wetting condition on rock surfaces is greatly influenced by the adsorption of organic components from the oils, either through physical or chemical alteration of the rock texture, thereby affecting oil flow, detachment, storage, and recovery.[43] Asphaltenes and resin fractions present in crude oil strongly adsorb onto clean rock surfaces and alter their wettability.[44] However, the extent of this effect may vary depending on the type of rock and oil used.[45] Studies on the adsorption of oil on different rock types have shown that quartz/sandstone rock adsorbs carboxylic acid ($2.76 \pm 0.19\ \mu mol/m^2$), kaolinite ($3.14 \pm 0.25\ \mu mol/m^2$), and calcite ($7.35 \pm 0.15\ \mu mol/m^2$), with calcite exhibiting the highest adsorption among the three considered. Nevertheless, the impact on other less attractive rock samples may still be significant for wettability alteration and should not be underestimated.[44,46] The surface charge density on rocks varies depending on the rock type and pH of the environment, which is an important aspect to consider in this study. It plays a significant role in the interaction between low-salinity ions and nonpolar hydrocarbons at the brine−oil interface. Therefore, it is crucial to focus on the interfacial tension behavior of brines such as NaCl and $CaCl_2$ in the presence of sodium dodecyl sulfate (SDS) based on this criterion. Nezhad et al. investigated the effects of interfacial tension for different brine solutions (Na_2SO_4, $CaCl_2$, $MgSO_4$, KCl, $CaSO_4$, NaCl, and $MgCl_2$) with crude oil and observed the changes in interfacial tension and contact angles when interacting with acidic crude oil. Understanding these phenomena requires the application of molecular dynamics (MD) simulation.[47]

Despite the wealth of existing research in this field, our study aims to provide additional insights into the molecular displacement occurring at both pore and subpore levels during oil displacement using a brine−surfactant solution. Our specific focus of this work is on elucidating the influence of cationic charges on contact angle alterations through a comprehensive analysis of relative concentration, with a particular emphasis on oil displacement on the quartz surface. Significantly, our observations reveal heightened adherence of polar oil beneath the surface, with more displacement occurring on the upper side

https://doi.org/10.1021/acsomega.4c00562
ACS Omega 2024, 9, 20277−20292

of the oil−brine interface, primarily attributed to the reduction in interfacial tension. The dynamic movement of oil molecules initially spreads on the rock surface under NaCl−SDS, as evidenced by prominent radial distribution peaks, diminishing as they are pulled off the surface. In contrast, the behavior observed with $CaCl_2$−SDS is the opposite. This contrast is attributed to the high charge on Ca^{2+}, leading to strong attachments to the quartz surface. In contact angle measurements, NaCl−SDS exhibited a reduction to 4−5° for concentrations ranging from 500 to 5000 ppm within 30 min, whereas $CaCl_2$−SDS showed a reduction to 4−6°. Notably, our investigation reveals that the cationic charge effect, polar oil, and brine−surfactant interactions have not been thoroughly explored in the context of oil detachment under low salinity conditions.

2. CHARGE CREATION ON SANDSTONE/QUARTZ SURFACE AND THEIR SIGNIFICANCE IN ELECTROSTATICS

The sandstone/quartz surface is composed of silanol groups (−Si−OH), which interact with hydroxyl (OH^-) or hydronium (H^+) ions from water via two processes: (i) when protons are adsorbed on the Si−OH surface under acidic conditions to form a positively charged surface, while under (ii) alkaline conditions, the surface of Si−OH deprotonates to form a negatively charged surface, as in eqs 1 and 2.[48]

$$\equiv\text{Si-OH} + H_3O^+ \leftrightarrow \equiv\text{Si-OH}_2^+ + H_2O \quad (1)$$

$$\equiv\text{Si-OH} + OH^- \leftrightarrow \equiv\text{Si-O}^- + H_2O \quad (2)$$

where $\equiv SiOH_2^+$, SiOH, and $\equiv SiO^-$represent the protonated surface, neutral, and deprotonated surface sites. The presence of more than one type of surface species implies that multiple reaction mechanisms can occur on the quartz surface during dissolution. However, the overall reactivity of the quartz surface depends on the relative distribution of the three species.[48,49] The chemistry of the quartz surface and the origin of negative charge are very important in the physical and chemical interactions of quartz with hydrophilic and hydrophobic molecules at all length scales for research and field engineering applications. This is the property that dictates the applicability of the quartz material for surface wettability studies. The adhesion and cohesion forces between the fluids of interest and the quartz surface depend on the surface charge density and fluids in contact.[48,50,51] The creation of negative charges is initiated by the deprotonation of silanol groups (≡Si−OH) on the surface of silica through a series of steps initiated as shown in eqs 3−5.[49]

$$\equiv\text{SiOH} \rightleftarrows \equiv\text{SiO}^- + H_S^+ \quad (3)$$

The amount of all the silanol groups per surface area, Γ_T (1/m^2), is $\Gamma_T = \Gamma_{SiOH} + \Gamma_{SiO^-}$, where Γ_{Si^-OH} is the amount of −Si−OH per surface area and Γ_{Si-O-} is the amount of SiO^- per surface area. The surface charge density, σ (C/m^2), is $\sigma = e\Gamma_{SiO^-}$, where e is the elementary charge. According to the law of mass action, $\frac{a^s_{H^+}\Gamma_{SiO^-}}{\Gamma_{SiOH}} = K = 10^{-pK}$, where K or 10^{-pK} is the dissociation constant and $a^s_{H^+}$(mol L^{-1}) is the activity of protons adjacent to the surface.

$$a^S_{H^+} = a_{H^+}\exp\left(\frac{-e\Psi_o}{k_BT}\right) \quad (4)$$

where a_{H^+} is the activity of proton in bulk solution, Ψ_0 is the surface potential (V); k_B is the Boltzmann constant, and T is the absolute temperature. The surface charge density is given by the following equations: $\sigma = C_s(\Psi_o - \Psi_d)$

$$\sigma = -\sigma_d = \left(\frac{2\varepsilon k K_B T}{e}\right)\sinh\left(\frac{e\Psi_d}{2K_BT}\right) \quad (5)$$

where C_S is the Stern layer capacitance (F/m^2); Ψ_d is the potential at the outer surface of the Stern layer (the diffuse layer potential); ε is the permittivity of the solvent (water) (F/m); κ is the Debye−Hückel parameter (m^{-1}); and σ_d is the charge density in the diffuse layer (C/m^2).[50,52,53] Studies have shown that three main interactions are possible when the polar components of crude oil are on rock surfaces, whereas acid−base and ion-binding interactions occur.[21,54−56] Due to these interactions, polar molecules are adsorbed on silicate rock surfaces by van der Waals forces or hydrogen bonding (negative disjoining pressure), thereby altering the hydrophilic original rock surface state to oil-wet.[57] Furthermore, the negatively charged acidic components cannot be adsorbed onto the negatively charged silicate rock because of electrostatic repulsion (positive disjoining pressure), which is helpful for oil recovery. The high-valent cations are found to bind the acidic components and rock surfaces via ion-binding interactions, taking advantage of the negatively charged rock surface exhibited by most sandstone rocks.[58−60] The increase in brine concentration of NaCl and $CaCl_2$ resulted in a decrease in negative zeta potentials for quartz/brine and oil/brine interfaces. Hua et al. showed that the highest negative charges were observed with rock/deionized water and oil/deionized water interfaces due to the dissociation of silanol groups on rock surfaces and carboxyl groups in oil. Increasing salinity of the NaCl solution resulted in compression of the electrical double-layer, which decreased the negative charges of the two interfaces. While with calcium ions, the effect of charge on two interfaces was more strongly attracted to the rock than that of Na^+ at the same ionic strength, a weak positive charge at the rock/brine interface and a weak negative charge at the oil/brine interface were observed at 63,603 ppm of $CaCl_2$ solution.[61] These results suggest that the ion composition and salinity are very important in determining the interactions between the rock/brine and oil/brine interfaces because they can strongly affect the electrical charge at both interfaces.[61] The influence of adhesion and cohesion forces on the solid−liquid interface was highlighted.[62−64] Oil−brine−rock systems, where brine films are confined between rocks and oil droplets, are found to depend on the characteristics of the rock surface, brine composition, and chemical properties of the oil droplets.[39] It is with the interest of this work to

1. Explore the low-salinity surfactant ion's interaction with oil on the charged quartz surface
2. Show low-salinity brine−surfactant hybrid interaction with the hydrophobic quartz surface at the atomistic level and subpore by contact angle and molecular simulations
3. Investigate the forces responsible for molecular oil adsorption and displacement using the sessile drop method and molecular dynamics simulation
4. Understand the low-salinity ranges which can be applied for research in a particular sandstone reservoir as a guiding principle since reservoirs are highly heterogeneous

To understand the molecular motion and dynamics of the decanoic acid/dodecane oil mixture on the quartz surface,

https://doi.org/10.1021/acsomega.4c00562
ACS Omega 2024, 9, 20277−20292

molecular dynamics (MD) simulations were conducted. These simulations played a crucial role in studying the interaction between brine, crude oil, and rock systems, which affect wettability by causing the dynamic adsorption of active components on the rock surface, leading to an oil-wet state.[8,65,66] Over the past few decades, MD simulations have emerged as a powerful tool for investigating complex interactions at a microscopic level, providing detailed information on the dynamic, energetic, and structural properties of these systems at the molecular scale. One of the applications of MD simulations is the study of oil interaction with quartz surfaces and detachment mechanisms.[67] Studies conducted by Mabudi et al. demonstrated that increasing the ionic concentrations of brine in the presence of *n*-decane resulted in decreased free energies and an increased wetting state of sandstone rocks.[68] Similar research by Jia et al. showed that the oil-wet quartz surface became more water-wet after removing adsorbed crude oil molecules using mixed surfactants. Contact angle measurements were performed to assess the effect of wettability alteration.[69] MD simulations offer valuable insights into the molecular-level behavior and interactions involved in low-salinity surfactant brine systems on quartz surfaces, providing a deeper understanding of wettability and detachment mechanisms in sandstone reservoirs.

3. MATERIALS AND METHODS

3.1. Materials. Chemicals used were sodium chloride (NaCl > 99.5%), calcium chloride anhydrous ($CaCl_2$, 99.99%), and sodium dodecyl sulfate ($C_{12}H_{35}OSO_3Na$ > 99.6%) purchased from Aladdin Chemical Reagent Company. All the chemicals were of analytical grade and used as received. Deionized water was used in all the experiments. Crude oil was obtained from the Shengli oilfield, whose composition and that of synthetic brine are given in Tables 1 and 2.

Table 1. Brine Compositions of Ions (ppm)

no	Na^+	Ca^{2+}	SDS	total salinity
1	49,750	49,750	250	50,000
2	29,750	29,750	250	30,000
3	9750	9750	250	10,000
4	4750	4750	250	5000
5	1750	1750	250	2000

Table 2. Crude Oil Composition

components	percentage (%)
aromatic hydrocarbons	31.13
resins	22.42
saturated hydrocarbons	36.12
asphaltenes	10.33

3.2. Experimental Procedure. The wettability alteration and oil displacement from the quartz surface were considered based on the interactions between the oil−brine−quartz/solid system using low-salinity surfactant application in two fronts: (1) based on contact angle variation by sessile drop experiment with varying low-salinity surfactant concentrations; (2) molecular dynamics simulation to study the dynamic displacement of (dodecanoic-dodecane) oil from the quartz surface using brine−surfactant. The dodecanoic-dodecane total acid number has a TAN value of 1.4 mg KOH/g) and crude oil has a TAN value of 1.1 mg KOH/g.[70]

3.2.1. Contact Angle Measurements.

1. Sandstone slices were cleaned with toluene, saturated with formation water, and aged in crude oil at 90 °C.[71,72]
2. Drops of brine−surfactant solutions of approximately 0.3 μL were delivered using a Hamilton syringe and carefully deposited on the surface of the oil-aged sandstone slices immersed in light crude oil for clear vision. Contact angle measurements were taken using the sessile drop method, and pictures were taken and recorded. Three readings were taken for each angle to obtain the average, and the procedure was repeated for other brine concentrations of 500, 1000, 10,000, 30,000, and 50,000 ppm. This was carried out for NaCl and $CaCl_2$.
3. Sodium dodecyl sulfate (8.2 Mm), which was of critical micelle concentration (CMC), was used.[73,74] The aged sandstone slices were placed in a vessel containing a dodecane−dodecanoic oil mixture, as shown in Figure 1.

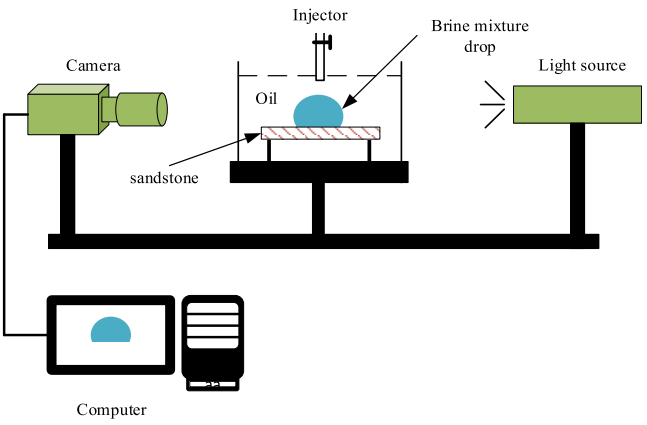

Figure 1. HARKE-SPCA schematic diagram of the experimental setup for contact angle measurement.

The images of the droplets were taken with a camera, and the contact angles were measured to ascertain the decreased angle at room temperature (25 °C) and pressure (1 atm).

3.2.2. Molecular Dynamics Simulation to Study Oil Removal by Low Salinity Water. In this simulation calculation, the condensed-phase optimized molecular potentials for atomistic simulation studies (COMPASS) force field in Materials Studio 2017 software was used for molecular dynamics simulation under the NVT ensemble at 303.1 K. The COMPASS force field is the first molecular force field that unifies organic and inorganic molecular systems and has been successfully utilized for asphalt and minerals such as quartz.[42,75−77] The α-quartz surface used was of dimension 3.93 × 6.81 × 2.0 nm^3, perpendicular to the *z*-axis from the surface. The silica surface is generated by cleaving the α-quartz structure along its 001 orientation and hydroxylated using hydroxyl with a density of 7.64 nm^{-2} to demonstrate the water-saturated rock. This was consistent with the results (5.9−18.8 nm^{-2}) calculated by Koretsky et al.[78] The amorphous cell was then constructed of 97 dodecane and 33 dodecanoic acid molecules geometrically optimized and combined with an optimized silica surface to form an adsorbed complex polar oil−quartz surface. Amorphous brine cells were constructed with 56 salt molecules for both NaCl and $CaCl_2$. They represented 1% of the total molecules in the cell of 5450. Higher concentrations

https://doi.org/10.1021/acsomega.4c00562
ACS Omega 2024, 9, 20277−20292

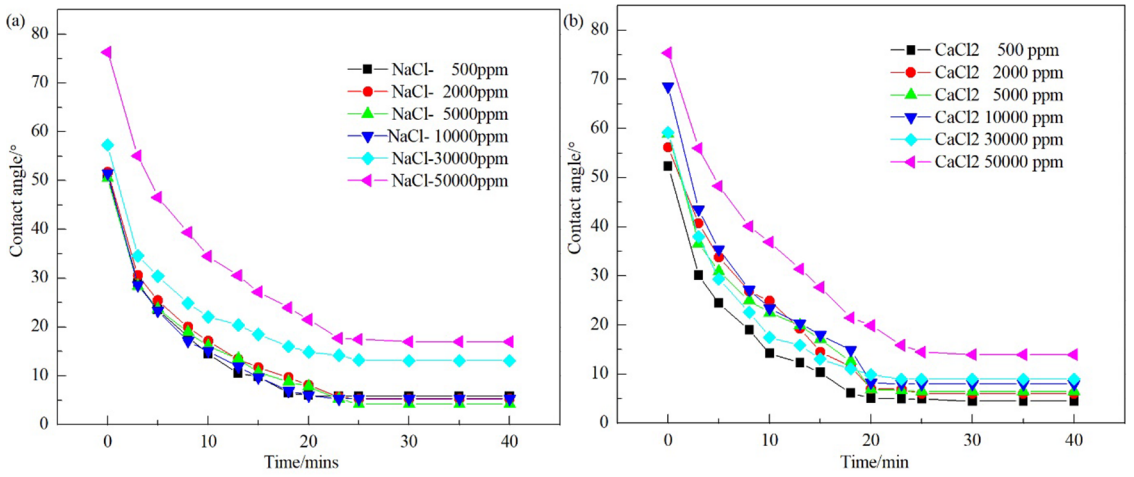

(a). Contact angles for low salinity brine: (a) NaCl-SDS and (b) $CaCl_2$-SDS

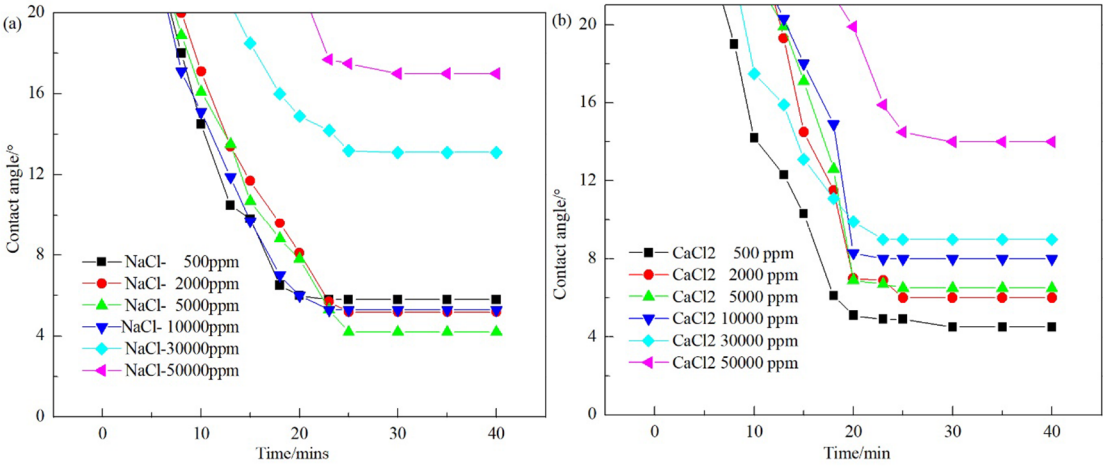

(b). Contact angles of variable concentrations of brine: (a) NaCl-SDS and (b) $CaCl_2$-SDS. (Magnified brine section for better vision)

Figure 2. (a) Contact angles for low-salinity brine: (a) NaCl−SDS and (b) $CaCl_2$−SDS. (b) Contact angles of variable concentrations of brine: (a) NaCl−SDS and (b) $CaCl_2$−SDS (magnified brine section for better vision).

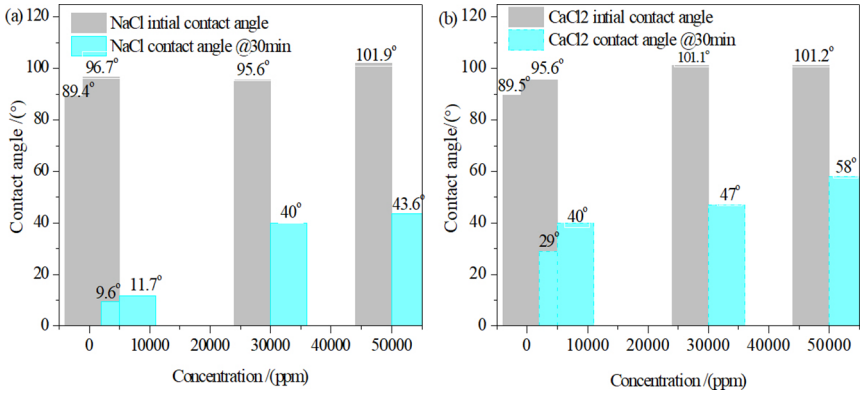

Figure 3. Histograms of initial and final contact angles of variable brine concentrations: (a) sodium chloride and (b) calcium chloride.

were considered too for 5, 10, and 25% with 273, 545, and 1363 salt molecules, respectively. The brine cells were each added 20 molecules of sodium dodecyl sulfate (SDS) and water molecules to make a total of 5450 in a cell.[35] The amorphous cells built were all geometrically optimized and relaxed by 2 ps of NPT before MD simulation at 303.1 K and 1 atm. Each low-salinity surfactant cell was combined with an oil−quartz surface and vacuum slab added to eliminate the effect of periodic boundary

https://doi.org/10.1021/acsomega.4c00562
ACS Omega 2024, 9, 20277−20292

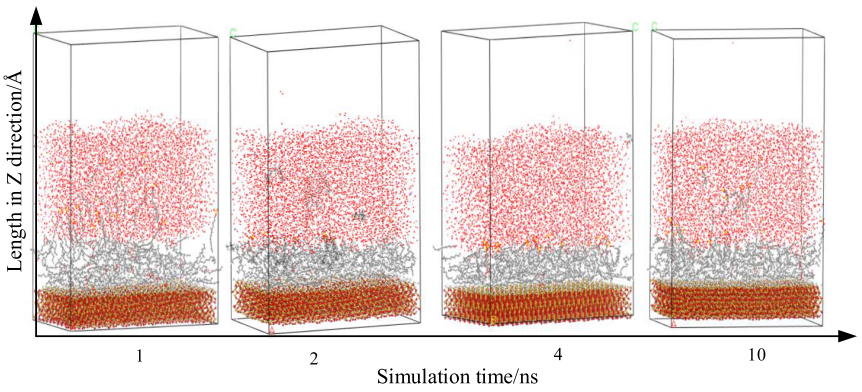

Figure 4. Synthetic polar oil displacement from quartz by 1% sodium chloride in (NaCl−SDS) brine.

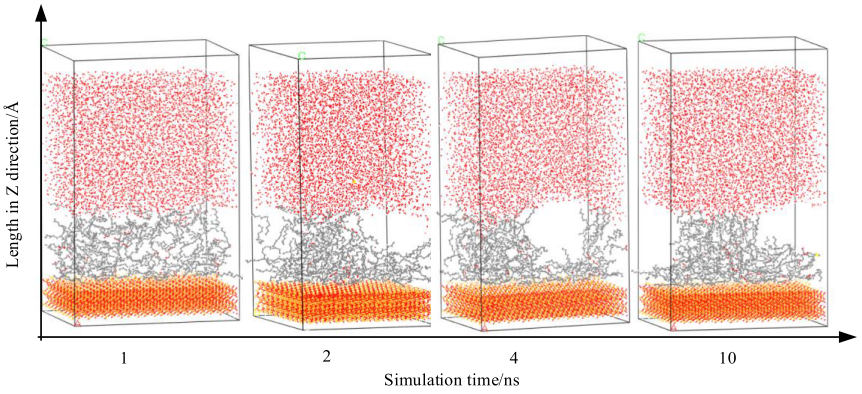

Figure 5. Synthetic polar oil displacement from the quartz surface by 1% sodium chloride (NaCl) brine.

conditions and geometrically optimized. Each cell underwent a 2 ps NPT MD simulation to remove bad contact between water and brine molecules. Then, varying NVT MD simulations were performed for every built slab at 303.1 K, with the silica surface being fixed in all calculations with a cutoff of 12.5 Å and a time step of 1 fs. Periodic boundary conditions were applied in all three dimensions. The optimization process involved utilizing the steepest descent method to optimize the atoms, cells, and quartz surface cells. Subsequently, a sequence of equilibrium molecular dynamics simulations spanning 1, 2, 4, and 10 ns was conducted to attain the equilibrium desorption configuration under the NVT ensemble at 303.1 K. This comprehensive procedure was executed for both low-salinity brine, with and without the surfactant. Following the NVT simulations, NPT simulations were performed at four distinct reservoir points characterized by varying temperatures and pressures: (303.14 K, 10 MPa), (323.14 K, 15 MPa), (343.14 K, 20 MPa), and (373.14 K, 30 MPa). The simulation parameters for the NPT were consistent with those employed in the NVT simulations.

4. RESULTS AND DISCUSSION

4.1. Graphs Showing the Rate of Change of Contact Angles for NaCl and $CaCl_2$ with Varying Ionic Concentrations. The results show the effects caused by decreased salinity, surfactant addition, and the residence time needed for wettability alteration to occur. It can clearly be seen that the increased salinity of brines causes a corresponding increase in contact angles on the sandstone surface. However, the addition of SDS surfactant to brines caused a highly noticeable reduction in contact angles compared to pure brines shown in Figures 2 and 3.

It is an illustration of how contact angles altered with varying concentrations for a period of 30 min for brines with and without the SDS surfactant. The influence of brine concentration on contact angle change was found to be more pronounced at higher concentrations (30,000−50,000 ppm) compared to the range of 1000−10,000 ppm. In Figure 2b, a section of the graph was enlarged to ensure better visualization of the data. When surfactants were added to the system, the contact angles decreased proportionally across all brine concentrations, indicating a consistent wetting behavior. However, relying solely on the macroscopic observations of contact angle reduction on the sandstone surface is insufficient for a comprehensive understanding of the wetting behavior of low-salinity brines. To gain a more realistic and detailed understanding, it is necessary to investigate atomic-level interactions and motions at the molecular level. This technique was used by Chang et al. to understand trapped oil in channels.[79] Molecular dynamics simulation has been proved to be an invaluable tool, as it provides a platform to study the wetting behavior of low-salinity surfactant flooding in conditions that closely resemble the experimental setup. By employing molecular dynamics simulation, we can examine the intricate dynamics of brine droplets on the sandstone surface, allowing a thorough analysis based on specific brine types and the influence of surfactants. The simulations considered variations in brine salinities and time frames, enabling a comprehensive investigation of the brine interaction with the sandstone surface and facilitating a more accurate analysis of the results. This approach helped in eliminating ambiguities that could occur in sessile drop experiments and significantly enhanced our understanding of various factors, including ion interactions with crude oil,

https://doi.org/10.1021/acsomega.4c00562
ACS Omega 2024, 9, 20277−20292

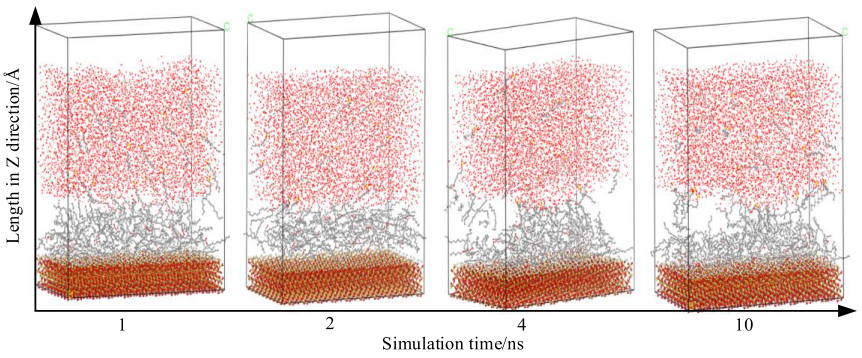

Figure 6. Synthetic polar oil displacement from the quartz surface by 1% calcium chloride in $CaCl_2$−SDS brine.

detachment, and displacement from the rock surface, as well as changes in wettability and improvements in oil recovery. The insights gained through molecular dynamics simulation play a crucial role in advancing our knowledge of these complex processes and can contribute to the development of more effective oil recovery techniques.

4.2. Effect of Cation Charge and Concentration on Contact Angles. In a study conducted by Wei et al. on the wettability of brine on quartz surfaces, it was observed that the wettability ranged from an intermediate wet state to a water-wet state. However, as the salt concentration was increased, the contact angles decreased to a nearly constant value. Moreover, further increases in the salt concentrations led to an increase in contact angles. These observations suggest that the quartz surface transitions to an oil-wet state at higher salt concentrations.[80] Different affinities were observed on quartz surfaces with the order of brine cation charge as follows: NaCl > $MgSO_4$ > $CaCl_2$ > $MgCl_2$. At high concentrations of brine, divalent cations such as Ca^{2+} and Mg^{2+} induce negative charges on the quartz surface. This phenomenon leads to the adsorption of these cations and the bridging of polar compounds present in the crude oil on the surface, as illustrated in Figure 5. The adsorption and bridging process is facilitated by the electrostatic effect, resulting in the adherence of organic species to the quartz surface.

The extra-high concentrations exhibited by the salt brines resulted in turning the quartz surface to be more oil-wet which increased the contact angles.[80]

These show that contact angles initially decreased and then increased as a result of an increased oil-wetting state on the quartz surface. The angle adjustment can be explained based on ionic strength and brine double-layer adjustment with expressions related in eqs 6 and 7.[80]

$$I = \frac{1}{2}\sum_j C_j Z_j^2 \tag{6}$$

where C is the molar concentration (mol/L) and z is the valence of ions. At low concentrations (<0.1 M), the thickness of the double layer, as measured by the Debye length (λ), is related to the ionic strength (I) of an electrolyte

$$\lambda = \left(\frac{\varepsilon K_B T}{1000 N_A e^2 I}\right)^{1/2} \tag{7}$$

where k_B is Boltzmann's constant (J/K), T is the temperature (K), ε is the permittivity of vacuum (F/m), N_A is Avogadro's number (mol^{-1}), and e is the charge on an electron. From the above two equations, the relationship between the brine thickness and ionic charge can be drawn. The thickness of an electrical double layer (λ) is inversely proportional to the ionic strength (I), and the decrease in ion strength is expected to produce a more water-wet surface. This is in line with double-layer expansion (DLE), suggesting a decrease in the contact angle. The ionic strength is inversely proportional to the double-layer thickness, i.e., higher attraction is encountered with higher ionic strength and cation charge. This double-layer expansion can be noticed by periodic changes in oil densities along the Z direction, which are found to vary according to concentrations and cation charge.

4.3. Investigation of Oil Detachment and Displacement from Quartz Surface by Sodium Chloride (NaCl) and Sodium Chloride−Surfactant (NaCl−SDS). During the simulation, in Figures 4 and 5, the oil displacement in the systems occurred under sodium chloride (NaCl) and sodium chloride with SDS surfactant (NaCl−SDS) brines. These molecular motions help us to understand the effect of ions and surfactant molecules on the removal of oil over time. The behavior of oil removal in these systems was observed by analyzing the distribution and concentration of oil molecules during the simulation.[81]

In the presence of NaCl, the interactions between Na^+ and Cl^- ions with the oil molecules and the surface of the system influenced the displacement of the oil. The presence of NaCl altered the interfacial tension and capillary pressure, leading to changes in the oil distribution within the system. This interaction between NaCl ions and oil molecules resulted in the migration and removal of oil from the system. Furthermore, the addition of SDS surfactant to the NaCl solution (NaCl−SDS system) had an additional impact on oil displacement. The surfactant molecules interacted with both the oil and the NaCl ions, modifying the interfacial properties and promoting the detachment of oil molecules from the system's surface. The presence of SDS surfactant enhanced the effectiveness of oil removal by reducing the interfacial tension and facilitating the dispersal of oil in the aqueous phase. Throughout the simulation, the changes in oil distribution and concentration were monitored to analyze the progress of oil displacement. The behavior of oil removal in the NaCl and NaCl−SDS systems was compared to understand the influence of the surfactant on the efficiency of oil removal. These findings provide valuable insights into the mechanisms underlying oil displacement in the presence of NaCl and SDS surfactants and can contribute to the development of strategies for enhanced oil recovery and reservoir management.

4.4. Investigation of Oil Detachment and Displacement from the Quartz Surface by Calcium Chloride

https://doi.org/10.1021/acsomega.4c00562
ACS Omega 2024, 9, 20277−20292

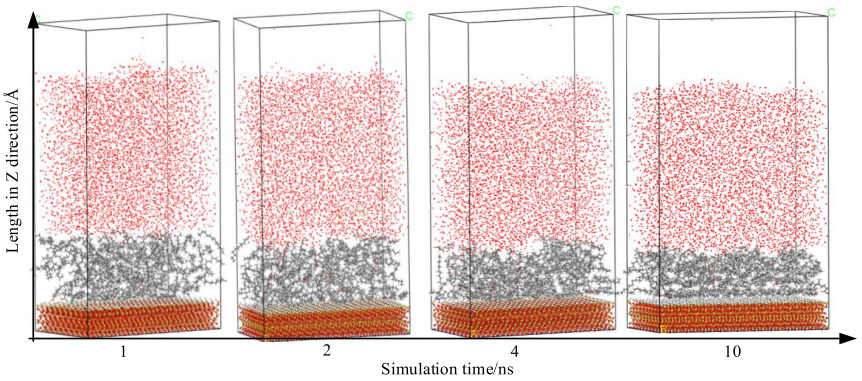

Figure 7. Optimum low-salinity brine of 1% $CaCl_2$ interaction with synthetic polar oil adsorbed on a quartz surface.

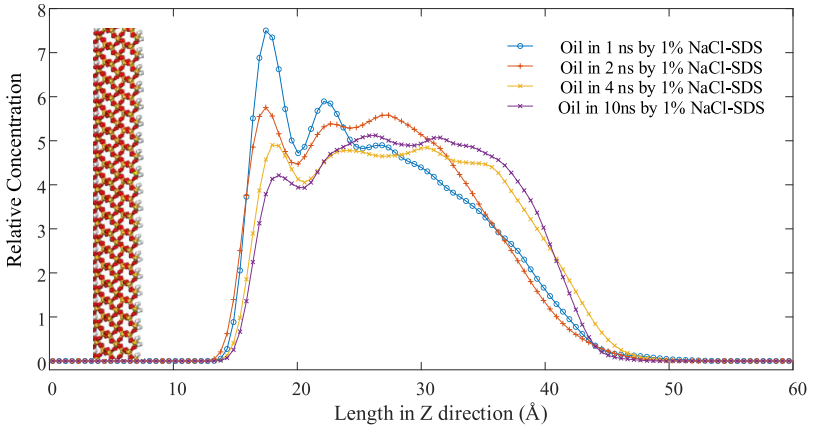

Figure 8. Relative concentration of dodecane (polar model oil) displacement from the quartz surface using NaCl−SDS.

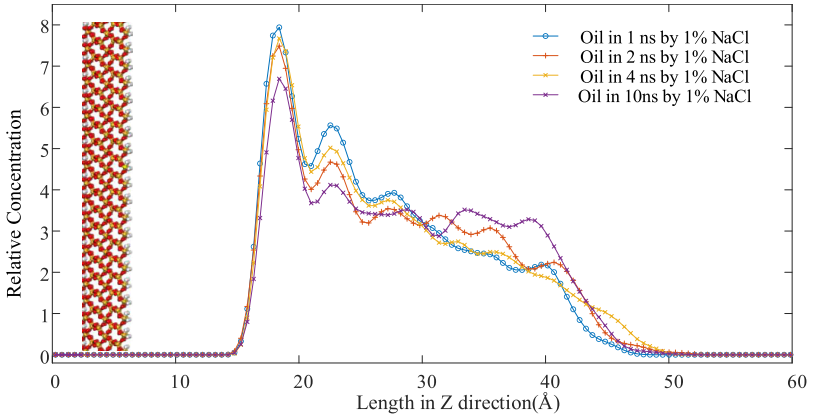

Figure 9. Relative concentration of dodecane (polar model oil) displacement from the quartz surface using NaCl.

($CaCl_2$) and Calcium Chloride−Surfactant ($CaCl_2$−SDS). The displacement of oil in the systems of calcium chloride ($CaCl_2$) and calcium chloride with the SDS surfactant ($CaCl_2$−SDS) is influenced by the presence of ions and surfactant molecules, as shown in Figures 6 and 7. In the system with calcium chloride alone, the ions play a crucial role in oil displacement.

Calcium ions (Ca^{2+}) have a higher affinity for the quartz surface compared to sodium ions (Na^+), which results in a stronger electrostatic attraction. This attraction between the calcium ions and the quartz surface enhances the detachment of oil molecules from the surface, leading to oil displacement.[82−84] Additionally, the presence of calcium ions can modify the interfacial tension between the oil and brine, facilitating the movement of oil through the system. When the SDS surfactant is introduced into the calcium chloride system ($CaCl_2$−SDS), the surfactant molecules interact with both the oil and brine phases, further influencing oil displacement. The surfactant molecules can adsorb onto the oil−brine interface, reducing the interfacial tension and promoting the formation of oil-in-water emulsions. This emulsification process aids in breaking down the oil into smaller droplets, making it easier for the oil to be dispersed and displaced by the brine. The presence of SDS surfactant can alter the wettability of the quartz surface. This renders the surface more water-wet, increasing the spreading of the brine and

https://doi.org/10.1021/acsomega.4c00562
ACS Omega 2024, 9, 20277−20292

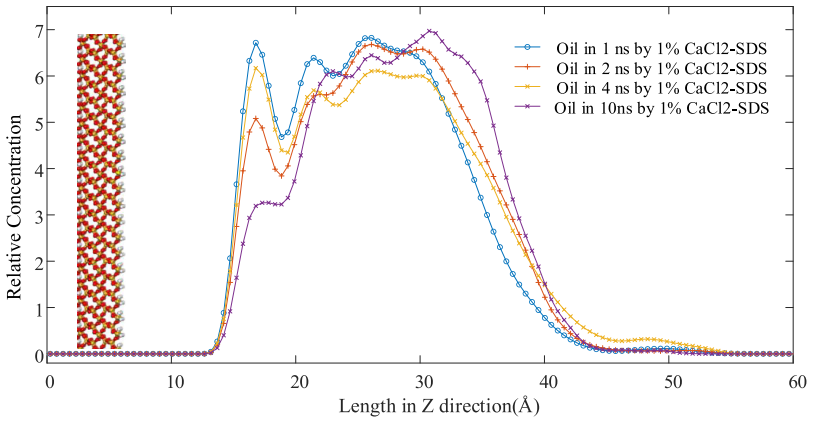

Figure 10. Relative concentration of dodecane (polar model oil) displacement from the quartz surface using $CaCl_2$−SDS brine.

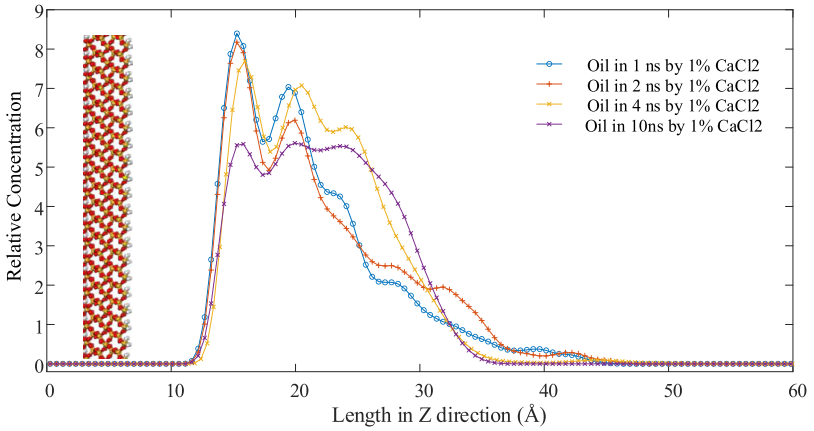

Figure 11. Relative concentration/density profile of dodecanoic acid−dodecane (polar model oil) variation from the quartz surface using $CaCl_2$ brine.

facilitating its penetration into the porous media, leading to enhanced oil displacement.[85]

4.5. Oil Detachment and Displacement from the Quartz Surface by NaCl and NaCl−SDS Solutions. The study investigated the impact of surfactant molecules, specifically NaCl−SDS, on the process of oil detachment compared with systems without surfactants. The amount of oil displaced from all of the systems was observed to be dependent on the residence time. Systems with longer residence times exhibited greater oil displacement, as shown in Figures 8 and 9.

The region of the oil−brine interface in the systems displayed a notable oil shift in the upper z direction from the surface. Notably, the NaCl−SDS interface demonstrated a higher degree of oil displacement compared with the $CaCl_2$−SDS interface. The NaCl system also exhibited more oil displacement compared to that of the $CaCl_2$ system. The method of relative concentrations was used by Mohammadali et al.[38] and Liu et al.[76] The inclusion of surfactants had a notable impact on the relative displacement of oil, leading to a more uniform shift compared with systems without surfactants. Figures 8 and 10 specifically illustrate the influence of the surfactant SDS at the interface between the two systems. These graphs are magnified at the top sides, indicating a pronounced bell-shaped pattern of oil displacement with NaCl−SDS. This behavior can be attributed to the reduction in interfacial tension caused by the presence of the surfactant. The surfactant enhances the viscoelasticity of the oil, resulting in a more significant displacement compared with low-salinity conditions alone, as shown in Figures 8 and 9. The molecular concentration analysis obtained from the simulations reveals that monovalent ions have the capability to detach oil molecules from the quartz surface. To simulate the presence of NaCl salt in low-salinity water, Na^{+}, and Cl^{-} ions were incorporated into the brine molecules, creating a brine layer within the simulation. A mass fraction of 1% w/w NaCl was utilized, involving the addition of 56 NaCl molecules to a total of 5450 molecules in the simulation cell. The equilibrium molecular distribution on the quartz surface and the relative concentrations of the molecules were examined to gain insights into the process of oil detachment from the rock surface. Initially, the molecular configurations of the models were equilibrated after the introduction of monovalent Na^{+} ions. This process involved the displacement of oil molecules from the quartz surface by water molecules, leading to the formation of a water film between the quartz surface and the oil molecules to be detached.

4.6. Oil Detachment and Displacement from the Quartz Surface by $CaCl_2$ and $CaCl_2$−SDS Solutions. Based on the calculations conducted using the models and the analysis of results in simulation cells, it can be concluded that the presence of Ca^{2+} ions contributed to the oil detachment process, although this occurred over an extended period of time. Figures 10 and 11 illustrate the equilibrium molecular distributions and the corresponding relative concentration profiles. The final molecular configurations observed at equilibrium after a certain duration in the models exhibited trends similar to those of the monovalent NaCl brine. In both cases, water molecules displaced the preadsorbed oil molecules from the quartz surface,

https://doi.org/10.1021/acsomega.4c00562
ACS Omega 2024, 9, 20277−20292

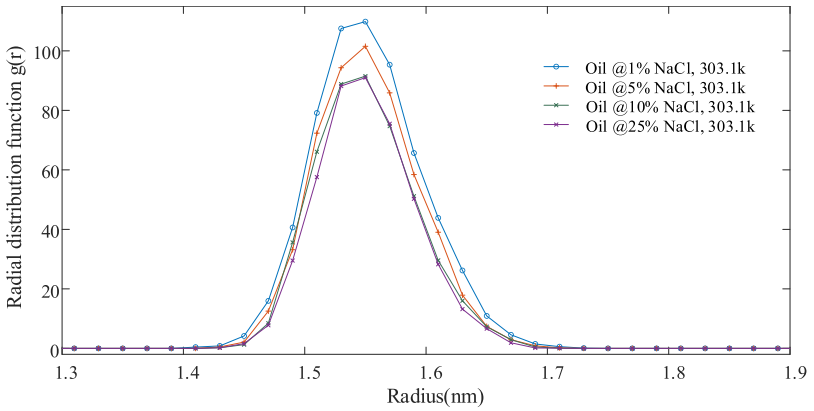

Figure 12. Radial distribution function of oil under varying NaCl concentrations at 303.1 K and 1 ns on the quartz surface.

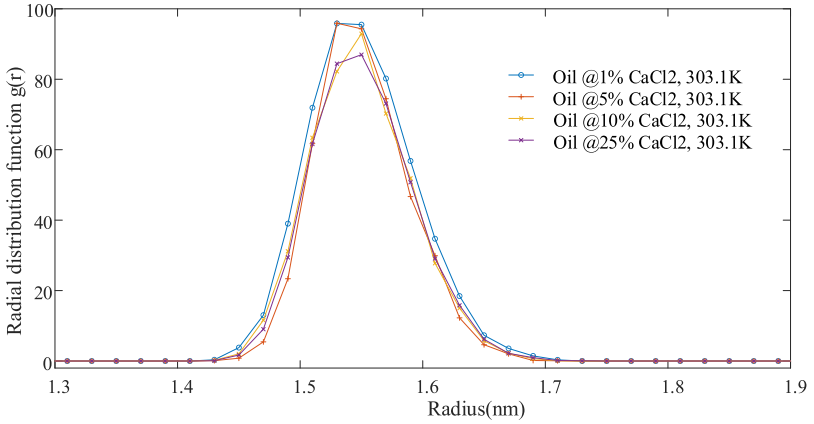

Figure 13. Radial distribution function of oil under varying $CaCl_2$ concentrations at 303.1 K and 1 ns on the quartz surface.

resulting in the accumulation of a water film between the oil molecules and the quartz surface.

The synthetic polar crude oil molecules in the models were gradually displaced by saline molecules and saline surfactant solutions, as indicated by the relative concentration distribution profiles shown in Figures 8−11. The process of detachment is slow, requiring longer residence times for significant oil detachment and displacement to occur. Promising results were observed from 20 ps onward for both NaCl and $CaCl_2$ brine systems, as well as for the NaCl−SDS and $CaCl_2$−SDS surfactant combinations. During the dynamic simulation of low-salinity conditions, the layered oil phase remained stable on the quartz surface, although the displacement of molecules varied depending on the type of brine and the duration of the simulation. The amount of displaced oil differed according to the brine type and the addition of surfactants. From the aforementioned figures, it can be observed that the SDS surfactant caused greater oil displacement in NaCl−SDS compared with the $CaCl_2$−SDS brine mixture. This can be attributed to the varying sizes of cations present in the two salts, which lead to different packing structures at the interface. The packing structure of the underlying oil layers exhibited slight changes that became more pronounced at lower brine concentrations. Mahmoudvand et al. also observed cation adsorption at the hydrocarbon−water interface, where the surface excess concentration was higher at low brine concentrations. Conversely, increased salt concentrations resulted in a higher bulk salt concentration and a reduction in surface excess, leading to an increase in interfacial tension.[86]

The analysis based on the Gibbs adsorption isotherm revealed that the top layer of the oil phase, which directly interacts with water molecules, undergoes more significant transformations during the simulation. The configuration of the top layer of dodecane, which represents the model oil, was observed to change according to studies conducted by refs 26,87,88 However, this trend exhibited variations at higher concentrations of $CaCl_2$−surfactant brine, primarily due to an increased rate of attraction between the oil layer and the surface.

4.7. Analysis of Results Using Radial Distribution Function (RDF). *4.7.1. Effect of Concentration on RDF of Oil in Different Brines.* The radial distribution function (RDF) is defined as the ratio of the density of a particular atom in the distance of r to the bulk density. In other words, the variation of density of a particular atom with a change in distance with reference molecules over the bulk density represents RDF. Therefore, it can be used to demonstrate a density distribution around a given molecule, and it is mathematically expressed as in eq 8[41]

$$g_{ab}(r) = \frac{V}{N_a N_b}\left(\sum_{i=1}^{N_a} \frac{n_i b(r)}{4\pi r^2 \Delta r}\right) \quad (8)$$

where N_a and N_b represent the total numbers of atoms a and b, respectively, V stands for the simulation box's volume, and $n_i b(r)$ denotes the number of atoms b at the radial distance of r from atom a for the peak closest to the rock surface. This is illustrated in Figures 12 and 13.

https://doi.org/10.1021/acsomega.4c00562
ACS Omega 2024, 9, 20277−20292

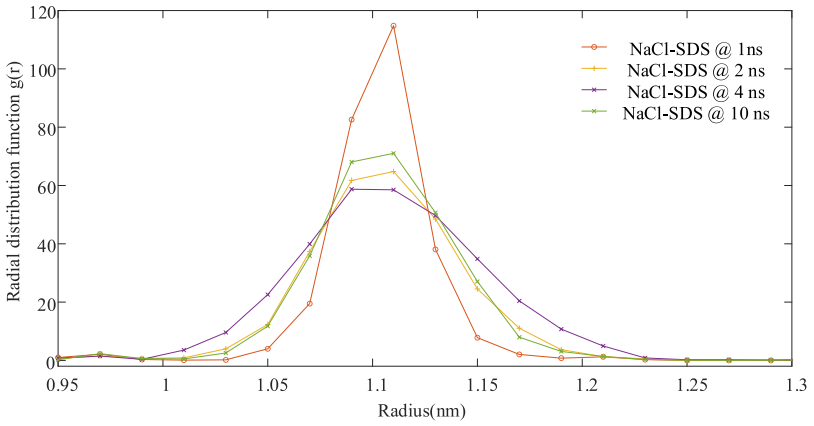

Figure 14. RDF of oil on a quartz surface under different simulation times with 1 wt % NaCl−SDS at 303.1 K.

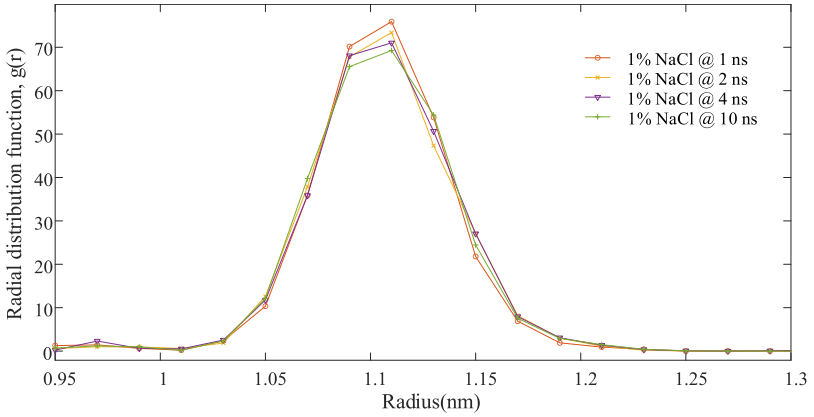

Figure 15. RDF of oil on a quartz surface under different simulation times with 1% w/w NaCl at 303.1 K.

Considering Figures 12 and 13, it can be observed that at low concentrations of NaCl and $CaCl_2$, the peaks in the radial distribution function of oil exhibit higher magnitudes. This phenomenon can be attributed to the intensified interactions between the oil molecules and the ions present in the low-concentration brine. In the case of low NaCl and $CaCl_2$ concentrations, the ionic species (Na^+ and Ca^{2+}) have a relatively lower number density in the solution. Consequently, these ions can approach the oil molecules more closely, resulting in more attractive interactions. The enhanced attractive forces between the oil molecules and the brine ions lead to higher RDF peaks, indicating an increased probability of oil desorption and potentially improved oil recovery. However, as the concentration of NaCl and $CaCl_2$ increases, the number density of the ionic species in the solution also rises. This higher concentration of ions causes the average distance between the oil molecules and ions to increase, thereby weakening the strength of the attractive interactions. As a result, the intensity of the RDF peaks decreases, suggesting a reduced likelihood of oil desorption and potentially lower oil recovery.

The observation of higher RDF peaks in the radial distribution function of oil at low concentrations of NaCl and $CaCl_2$ suggests the presence of stronger attractive interactions between the oil and ions, which may enhance the likelihood of oil desorption and potentially lead to improved oil recovery. Conversely, as the concentration of NaCl and $CaCl_2$ increases, the weaker interactions contribute to lower RDF peak magnitudes, indicating a decreased probability of oil desorption and potentially lower oil recovery. At the highest concentration of >1% NaCl and $CaCl_2$, it is observed that the RDF exhibits the highest peaks. This can be attributed to the relatively lower number density of the ionic species (Na^+ and Ca^{2+}) in solution at this concentration. As a result, the ions can approach the oil molecules more closely, leading to stronger attractive interactions. These intensified interactions result in higher RDF peaks, indicating a greater likelihood of oil desorption and potentially improved oil recovery. On the other hand, as the concentrations of NaCl and $CaCl_2$ increase to 5, 10, and 25%, the number density of the ionic species in the solution also increases. This higher concentration of ions results in a larger average distance between the oil molecules and ions, weakening the strength of the attractive interactions. Consequently, the intensity of the RDF peaks decreases for these higher concentrations, suggesting a reduced probability of oil desorption and a potentially lower oil recovery.

4.7.2. Influence of Simulation Time and Surfactant on RDF of Oil in Brine and Brine−Surfactant Systems. The variation in peaks observed in the radial distribution functions (RDFs) of NaCl, NaCl−SDS, $CaCl_2$, and $CaCl_2$−SDS reflects the different molecular arrangements and interactions in the systems.[89,90] These peaks indicate the probability of finding oil molecules at specific distances from the brine and brine−surfactant molecules. The observation of higher peaks in a short time for NaCl and NaCl−SDS systems compared to a lengthy time can be attributed to the dynamics of molecular interactions and the kinetics of oil detachment processes.

In the early stages of the simulation, when the NaCl and NaCl−SDS systems are introduced, there is a rapid exchange of

https://doi.org/10.1021/acsomega.4c00562
ACS Omega 2024, 9, 20277−20292

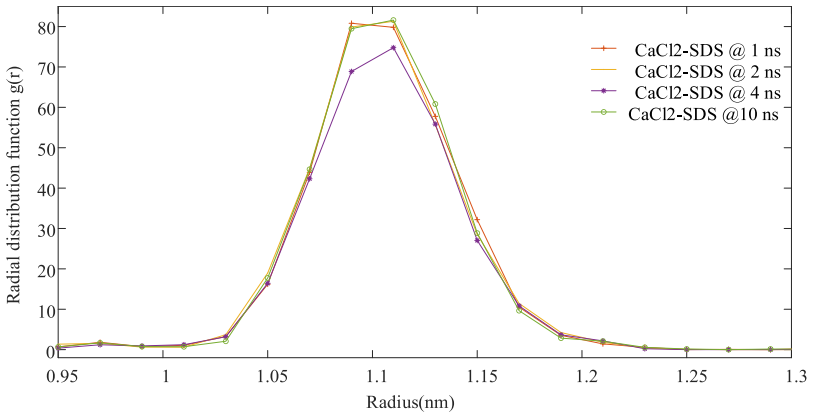

Figure 16. RDF of oil on the quartz surface under different simulation times with 1% w/w $CaCl_2$−SDS at 303.1 K.

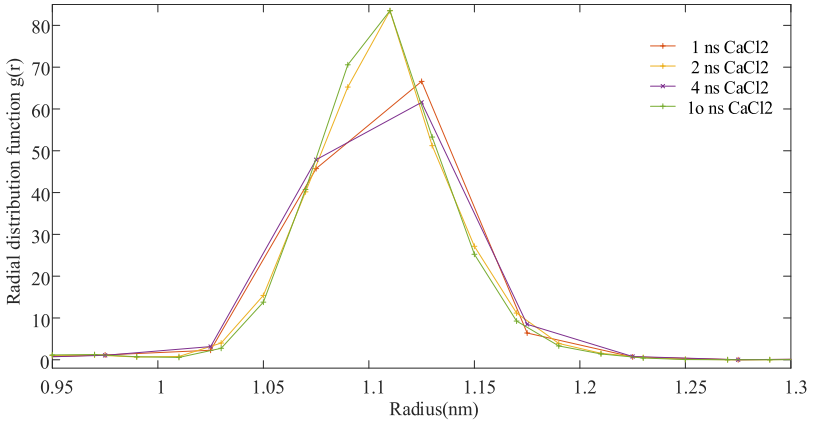

Figure 17. RDF of oil on the quartz surface under different simulation times with 1% w/w $CaCl_2$ at 303.1 K.

ions and the establishment of an equilibrium state between the oil and the brine and surfactant molecules for low-salinity brine. This initial exchange and equilibration process can lead to the formation of closer molecular arrangements and stronger interactions between the oil and brine/surfactant molecules. As a result, higher peaks are observed in the radial distribution functions (RDF) at shorter distances. This phenomenon is reported as the orientation and change in distance for oil molecules on the quartz surface.[91]

In the early stages, the repulsive forces between the brine/surfactant molecules and the oil may dominate, leading to a more efficient detachment of oil from the quartz surface and resulting in higher peaks in the RDF. However, as time progresses, an equilibrium between attractive and repulsive forces may be established, leading to a decrease in the amplitude of the peaks, as shown in Figures 14 and 15.

On the contrary, the behavior of $CaCl_2$ and $CaCl_2$−SDS systems in terms of the variation in peaks of RDFs and their influence on oil detachment from the quartz surface can differ from NaCl and NaCl−SDS systems. The longer oil radial distribution peaks were obtained for $CaCl_2$ and $CaCl_2$−SDS systems in 10 ns of 80 g/cm^3 and 70 g/cm^3 for 1 ns with the surfactant and varied in the absence of surfactant. This could be attributed to the complex interactions between the oil molecules and the surrounding brine/surfactant molecules. The divalent cations (Ca^{2+}) and the surfactant molecules can form stronger associations with the oil molecules compared with monovalent systems. These associations can result in the formation of larger aggregates or clusters of oil molecules surrounded by the brine/surfactant molecules. over a longer time, and these aggregates or clusters of oil molecules have more opportunity to stabilize and reach a state of equilibrium. This leads to the persistence of the oil radial distribution peaks for a longer duration, indicating a longer range correlation between the oil and the surrounding molecules. Therefore, the longer oil radial distribution peaks observed in $CaCl_2$ and $CaCl_2$−SDS systems after a longer time indicate a more persistent and stable arrangement of the oil molecules with the brine/surfactant molecules, as shown in Figures 16 and 17.

4.8. Effect of Brine−Surfactant Ions on Oil Movement and Detachment from Pores. *4.8.1. Utilizing Total Disjoining Pressure in Low Salinity to Determine Oil Desorption and Adsorption.* The two brines calcium chloride and sodium chloride exhibit different forces under different concentrations on the quartz surface. The dynamic motion of oil between quartz−brine and brine between quartz−oil was investigated by Wu et al. using two brines, sodium chloride and calcium chloride, at the same conditions. They observed that brines at different concentrations encountered varying attractive and repulsive forces as a result of intermolecular forces which comprised primarily of van der Waals, electrical, and structural forces.[86]

The molecular motion within the simulation box happens depending on whether the total disjoining pressure is positive or negative. When low concentrations of sodium chloride and calcium chloride concentrations of 1 wt % were considered, positive disjoining pressure occurred as explained above during the MD simulation. The results analyzed can be compared to the

https://doi.org/10.1021/acsomega.4c00562
ACS Omega 2024, 9, 20277−20292

relative oil concentrations displaced along the *Z*-direction. However, negative total disjoining pressure is expected at high concentrations and ionic attraction, which occurs in the stern layer next to the rock surface. For NaCl−SDS and $CaCl_2$−SDS brines, the surfactant gets adsorbed at the oil−brine interface resulting in decreased interfacial tension. This phenomenon has been reported by other scholars. The surface-active compounds from crude oil such as asphaltenes and naphthenic acids attract cations at the interface, leading to a reduction in the surface excess concentration and interfacial tension at low brine concentrations.[92] This adsorption reaches a minimum, followed by desorption, and ions start getting deposited in the brine bulk, leading to the quartz surface getting oil-wet. This results in a positive total disjoining pressure.[16,30,93] The negative and positive disjoining pressures represent contractive and repulsive forces, respectively.[56] This positive total pressure resulted in oil displacement and, consequently, oil molecules getting detached from the rock surface, as shown by molecular simulation.

4.8.2. Effect of Reduction in Interfacial Tension at the Oil−Brine Interface. Oil displacement occurs within the simulation cell when the brine percolates to the rock surface, creating a thin film that interacts with the oil adsorbed on the rock surface. This film responds electrostatically according to the total disjoining pressure. If the total disjoining pressure is positive, it exerts a repulsive force, pushing the oil away from the rock surface and causing oil displacement. Conversely, a negative total disjoining pressure leads to the adsorption of oil on the rock surface. The observed oil displacement over time at various brine concentrations, as depicted in Figures 4−7, demonstrates the presence of a repulsive force originating from the quartz surface. As time progresses, interactions between crude oil and brine result in the transfer of ions to the crude oil−brine interface, leading to changes in ion concentration both in the bulk solution and at the interface. This phenomenon is known as the concentration of the free surface energy. Increasing the brine concentration gradually results in a decrease in contact angles until a certain salinity limit is reached, beyond which the contact angles begin to increase. At minimal interfacial tension, the contact angles are reduced. This behavior aligns with the principles of the Gibbs adsorption isotherm, which describes the relationship between the changes in interfacial tension and alterations in the chemical activity of solution components, including ions in the bulk solution and at the interface, as described by eq 9[94,95].

$$d\gamma = -RT \sum \Gamma_n d\ln a_n \tag{9}$$

where $d\gamma$ is the change in interfacial tension, R presents the universal gas constant, T denotes the absolute temperature, and Γ_n and a_n stand for the surface excess concentration and the chemical activity of the nth component in the solution, respectively.[94]

The decrease in NaCl concentration causes expansion of the electrical double layer and greater repulsive forces between oil/brine and rock/brine; this is due to the more negative surface charge created on the rock surface which repels the co-ions associated with low-salinity brine, creating a favorable surface for oil detachment. For higher brine concentrations like in formation water, cations in this brine get attracted to negatively charged sites on the rock surface and negatively charged polar groups at the oil−water interface, which causes electrostatic attraction to occur. The bridge is created between the rock surface and the oil−water interface, and as a consequence, the rock surface becomes more oil-wet. However, low salinity helps to dislodge the adsorbed oil, leading to detachment and increased oil recovery.

4.8.3. Effect of Low-Salinity Brine pH on Oil Desorption. The pH of injected low-salinity water significantly impacts the protonation of sandstone rock surfaces in brine with varying ion compositions, thereby influencing the surface charges of minerals and organic compounds. Silica surface charges are notably pH-dependent, being negatively charged at higher pH (7.5−10) due to silanol group ionization. In the pH range of 3−7.5, surface charges exhibit slight pH dependence, with positive charges resulting from H^+ ion adsorption below pH 3.95. Reservoir brines, typically above the isoelectric point (pH = 2−2.5) on silicates, lead to negatively charged surfaces. The pH of injected water is pivotal in determining the surface chemical group composition and organic compound polar group distribution. In crude oil, diverse forces like van der Waals, hydrogen bonds, Coulombic, and surface forces interact intricately with the rock surface and organic compound groups. Consequently, attraction between polar groups and rock surfaces weakens, with hydrogen-bond interactions inducing electrostatic repulsion, while Coulombic forces strengthen, leading to organic compound desorption and enhanced rock surface hydrophilicity. Adsorption and desorption sensitivity to pH changes brought by low-salinity brine are particularly pronounced on clay mineral surfaces.

5. CONCLUSIONS

1. Low-salinity brine ranging from 500 to 5000 ppm resulted in the most notable reduction in contact angles, indicating significant wettability alteration after 30 min. In alignment with molecular dynamics simulations, low-salinity brines exhibited the highest radial distribution curves, highlighting stronger adhesion forces compared to cohesion at lower salinities, consequently leading to a higher rate of radial diffusion for both NaCl and $CaCl_2$ brines.

2. The dynamic movement of oil molecules initially spreads on the rock surface under NaCl−SDS, as indicated by prominent radial distribution peaks, and subsequently diminishes as they are pulled off the surface. In contrast, the behavior observed with $CaCl_2$−SDS is the opposite. This discrepancy is attributed to the high charge on Ca^{2+}, which forms strong attachments to the quartz surface.

3. At the oil−brine interface, the interaction between oil molecules and the surfactant (sodium dodecyl sulfate) resulted in a distinctive bell-shaped curve shift, as evident from the relative concentration curves. This phenomenon was notably less pronounced in pure brines without the presence of the surfactant.

4. The mechanism of low-salinity enhanced oil recovery (EOR) is proposed to illustrate the process wherein polar oil adheres to the rock surface. However, in the presence of low salinity, oil desorption occurs, resulting in improved oil displacement and enhanced oil recovery.

5. Low-salinity surfactant solutions are very important in reducing interfacial tension, and penetration potential into the thin film by the electrokinetic potential gradient results in increased detachment by positive disjoining pressure at low salinity.

https://doi.org/10.1021/acsomega.4c00562
ACS Omega 2024, 9, 20277−20292

AUTHOR INFORMATION

Corresponding Author

Renyuan Sun − *School of petroleum Engineering, China University of Petroleum (East China), Qingdao 0086, China*; Email: sunry@upc.edu.cn

Authors

Ernest Peter Maiki − *School of petroleum Engineering, China University of Petroleum (East China), Qingdao 0086, China*; orcid.org/0009-0003-0108-3805

Shaoran Ren − *School of petroleum Engineering, China University of Petroleum (East China), Qingdao 0086, China*

Ayman Mutahar AlRassas − *School of petroleum Engineering, China University of Petroleum (East China), Qingdao 0086, China*; orcid.org/0000-0002-7539-1865

Complete contact information is available at: https://pubs.acs.org/10.1021/acsomega.4c00562

Funding

This research did not receive any specific grant from funding agencies in the public, commercial, or any for-profit sectors.

Notes

The authors declare no competing financial interest.

ACKNOWLEDGMENTS

The authors thank China University of Petroleum for financing their PhD studies and Makerere University for granting them study leave to embark on the studies.

REFERENCES

(1) Bernard, G. G.Effect of Floodwater Salinity on Recovery Of Oil from Cores Containing Clays. In *Soc. Pet. Eng.*; 1967.

(2) Austad, T.; RezaeiDoust, A.; Puntervold, T.Chemical Mechanism of Low Salinity Water Flooding in Sandstone Reservoirs. In *Proc. - SPE Symp. Improv. Oil Recovery*; 2010; Vol. *1*, pp 679−695.

(3) Elakneswaran, Y.; Ubaidah, A.; Takeya, M.; Shimokawara, M.; Okano, H. Effect of Electrokinetics and Thermodynamic Equilibrium on Low-Salinity Water Flooding for Enhanced Oil Recovery in Sandstone Reservoirs. *ACS Omega* **2021**, *6*, 3727−3735.

(4) Akai, T.; Alhammadi, A. M.; Blunt, M. J.; Bijeljic, B. Mechanisms of Microscopic Displacement During Enhanced Oil Recovery in Mixed-Wet Rocks Revealed Using Direct Numerical Simulation. *Transp. Porous Media* **2019**, *130*, 731−749.

(5) Nasralla, R. A.; Mahani, H.; van der Linde, H. A.; Marcelis, F. H. M.; Masalmeh, S. K.; Sergienko, E.; Brussee, N. J.; Pieterse, S. G. J.; Basu, S. Low Salinity Waterflooding for a Carbonate Reservoir: Experimental Evaluation and Numerical Interpretation. *J. Pet. Sci. Eng.* **2018**, *164*, 640−654.

(6) Nasralla, R. A.; Nasr-El-Din, H. A.Coreflood Study of Low Salinity Water Injection in Sandstone Reservoirs. In *Soc. Pet. Eng. - SPE/DGS Saudi Arab. Sect. Technol. Symp. Exhib. 2011*; 2018; pp 187−199.

(7) Ligthelm, D. J.; Gronsveld, J.; Hofman, J. P.; Brussee, N. J.; Marcelis, F.; Van Der Linde, H. A.Novel Waterflooding Strategy by Manipulation of Injection Brine Composition. In *Soc. Pet. Eng. - Eur. Conf. Exhib.*; 2009; Vol. *2009*, pp 1− 22.

(8) Teklu, T. W.; Alameri, W.; Kazemi, H.; Graves, R. M.; AlSumaiti, A. M. Low Salinity Water−Surfactant−CO2 EOR. *Petroleum* **2017**, *3*, 309−320.

(9) Liu, S.*Alkaline Surfactant Polymer Enhanced Oil Recovery Process*; 2007; pp 1−222 .

(10) Zivar, D.; Pourafshary, P.; Moradpour, N. Capillary Desaturation Curve: Does Low Salinity Surfactant Flooding Significantly Reduce the Residual Oil Saturation? *J. Pet. Explor. Prod. Technol.* **2021**, *11*, 783−794.

(11) Almahfood, M. Experimental Study on a Novel Eor Method − Polymeric Nanogel Combined With Surfactant and Low Salinity Water Flooding To Enhance Oil Recovery. *Dissertation* **2020**.

(12) Alizadehmojarad, A. A.; Fazelabdolabadi, B.; Vuković, L. Surfactant-Controlled Mobility of Oil Droplets in Mineral Nanopores. *Langmuir* **2020**, *36*, 12061−12067.

(13) Dabiri, A.; Honarvar, B. Synergic Impacts of Two Non-Ionic Natural Surfactants and Low Salinity Water on Interfacial Tension Reduction, Wettability Alteration and Oil Recovery: Experimental Study on Oil Wet Carbonate Core Samples. *Nat. Resour. Res.* **2020**, *29*, 4003−4016.

(14) Jing, W.; Fu, S.; Zhang, L.; Li, A.; Ren, X.; Xu, C.; Gao, Z. Pore Scale Experimental and Numerical Study of Surfactant Flooding for Enhanced Oil Recovery. *J. Pet. Sci. Eng.* **2021**, *196*, No. 107999.

(15) Alrassas, A. M.; Vo Thanh, H.; Ren, S.; Sun, R.; Al-Areeq, N. M.; Kolawole, O.; Hakimi, M. H. CO2Sequestration and Enhanced Oil Recovery via the Water Alternating Gas Scheme in a Mixed Transgressive Sandstone-Carbonate Reservoir: Case Study of a Large Middle East Oilfield. *Energy Fuels* **2022**, *36*, 10299.

(16) Liu, F.; Wang, M. Review of Low Salinity Waterflooding Mechanisms: Wettability Alteration and Its Impact on Oil Recovery. *Fuel* **2020**, *267*, No. 117112.

(17) Derikvand, Z.; Rezaei, A.; Parsaei, R.; Riazi, M.; Torabi, F. A Mechanistic Experimental Study on the Combined Effect of Mg2+, Ca2+, and SO42- Ions and a Cationic Surfactant in Improving the Surface Properties of Oil/Water/Rock System. *Colloids Surfaces A Physicochem. Eng. Asp.* **2020**, *587*, No. 124327.

(18) Wang, X.; Alvarado, V. Effects of Low-Salinity Waterflooding on Capillary Pressure Hysteresis. *Fuel* **2017**, *207*, 336−343.

(19) Bai, Y.; Sui, H.; Liu, X.; He, L.; Li, X.; Thormann, E. Effects of the N, O, and S Heteroatoms on the Adsorption and Desorption of Asphaltenes on Silica Surface: A Molecular Dynamics Simulation. *Fuel* **2019**, *240*, 252−261.

(20) Lager, A.; Webb, K. J.; Black, C. J. J.; Singleton, M.; Sorbie, K. S. Low Salinity Oil Recovery - An Experimental Investigation. *Petrophysics* **2008**, *49*, 28−35.

(21) Tian, H.; Wang, M. Electrokinetic Mechanism of Wettability Alternation at Oil-Water-Rock Interface. *Surf. Sci. Rep.* **2017**, *72*, 369−391.

(22) Omekeh, A. V.; Friis, H. A.; Evje, S.; Fjelde, I. A Model for Low Salinity Flooding Experiments: Dissolution and Ion Exchange. *J. Porous Media* **2015**, *18*, 189−213.

(23) Chen, Q.; Otaibi, M.; Ayirala, S.; Yousef, A. The Prospects and Potential Opportunities of Low Salinity Water Flooding for Offshore Applications in Sandstones. *J. Pet. Sci. Eng.* **2021**, *199*, No. 108260.

(24) Guo, H.; Nazari, N.; Esmaeilzadeh, S.; Kovscek, A. R. A Critical Review of the Role of Thin Liquid Films for Modified Salinity Brine Recovery Processes. *Curr. Opin. Colloid Interface Sci.* **2020**, *50*, No. 101393.

(25) Mugele, F.; Bera, B.; Cavalli, A.; Siretanu, I.; Maestro, A.; Duits, M.; Cohen-Stuart, M.; Van Den Ende, D.; Stocker, I.; Collins, I. Ion Adsorption-Induced Wetting Transition in Oil-Water-Mineral Systems. *Sci. Rep.* **2015**, *5*, 1−8.

(26) Tetteh, J. T.; Barimah, R.; Korsah, P. K. Ionic Interactions at the Crude Oil-Brine-Rock Interfaces Using Different Surface Complexation Models and DLVO Theory: Application to Carbonate Wettability. *ACS Omega* **2022**, *7*, 7199−7212.

(27) Yue, L.; Pu, W.; Zhao, S.; Zhang, S.; Ren, F.; Xu, D. Insights into Mechanism of Low Salinity Water Flooding in Sandstone Reservoir from Interfacial Features of Oil/Brine/Rock via Intermolecular Forces. *J. Mol. Liq.* **2020**, *313*, No. 113435.

(28) AlRassas, A. M.; Vo Thanh, H.; Ren, S.; Sun, R.; Le Nguyen Hai, N.; Lee, K. K. Integrated Static Modeling and Dynamic Simulation Framework for CO_2 Storage Capacity in Upper Qishn Clastics, S1A Reservoir, Yemen. *Geomech. Geophys. Geo-Energy Geo-Resour.* **2022**, *8*, 2.

(29) Al-khafaji, A. A. H. *Multi-Scale Investigation of Low Salinity Water Flooding for Enhanced Oil Recovery Submitted in Accordance with the*

Requirements for the Degree of Doctor of Philosophy The University of Leeds School of Chemical and Process Engineering; 2019.
(30) Chandrasekhar, B.; Rao, D.Application of DLVO Theory to Characterize Spreading in Crude Oil-Brine-Rock Systems. In *SPE*; 2007.
(31) Sorbie, K. S.; Collins, I. R.A Proposed Pore-Scale Mechanism for How Low Salinity Waterflooding Works. In *SPE - DOE Improv. Oil Recover. Symp. Proc.*; 2010; Vol. *1*, pp 760−777.
(32) Ambekar, A. S.; Mattey, P.; Buwa, V. V. Pore-Resolved Two-Phase Flow in a Pseudo-3D Porous Medium: Measurements and Volume-of-Fluid Simulations. *Chem. Eng. Sci.* **2021**, *230*, No. 116128.
(33) Lebedeva, E. V.; Fogden, A. Micro-CT and Wettability Analysis of Oil Recovery from Sand Packs and the Effect of Waterflood Salinity and Kaolinite. *Energy Fuels* **2011**, *25*, 5683−5694.
(34) Al-Obaidi, D. A.; Al-Mudhafar, W. J.; Al-Jawad, M. S. Experimental Evaluation of Carbon Dioxide-Assisted Gravity Drainage Process (CO2-AGD) to Improve Oil Recovery in Reservoirs with Strong Water Drive. *Fuel* **2022**, *324*, No. 124409.
(35) Tang, J.; Qu, Z.; Luo, J.; He, L.; Wang, P.; Zhang, P.; Tang, X.; Pei, Y.; Ding, B.; Peng, B.; et al. Molecular Dynamics Simulations of the Oil-Detachment from the Hydroxylated Silica Surface: Effects of Surfactants, Electrostatic Interactions, and Water Flows on the Water Molecular Channel Formation. *J. Phys. Chem. B* **2018**, *122*, 1905−1918.
(36) Tian, H.; Wang, M. Molecular Dynamics for Ion-Tuned Wettability in Oil/Brine/Rock Systems. *AIP Adv.* **2017**, *7*, 125017.
(37) Liu, Q.; Yuan, S.; Yan, H.; Zhao, X. Mechanism of Oil Detachment from a Silica Surface in Aqueous Surfactant Solutions: Molecular Dynamics Simulations. *J. Phys. Chem. B* **2012**, *116*, 2867−2875.
(38) Ahmadi, M.; Chen, Z. Molecular Dynamics Simulation of Oil Detachment from Hydrophobic Quartz Surfaces during Steam-Surfactant Co-Injection. *Energy* **2022**, *254*, No. 124434.
(39) Khosravi, V.; Mahmood, S. M.; Zivar, D.; Sharifigaliuk, H. Investigating the Applicability of Molecular Dynamics Simulation for Estimating the Wettability of Sandstone Hydrocarbon Formations. *ACS Omega* **2020**, *5*, 22852−22860.
(40) Underwood, T. R.; Greenwell, H. C. The Water-Alkane Interface at Various NaCl Salt Concentrations: A Molecular Dynamics Study of the Readily Available Force Fields. *Sci. Rep.* **2018**, *8*, 1−12.
(41) Yu, T.; Li, Q.; Hu, H.; Tan, Y.; Xu, L. Molecular Dynamics Simulation of the Interfacial Wetting Behavior of Brine/Sandstone with Different Salinities. *Colloids Surfaces A Physicochem. Eng. Asp.* **2022**, *632*, No. 127807.
(42) Remesal, E. R.; Suárez, J. A.; Márquez, A. M.; Sanz, J. F.; Rincón, C.; Guitián, J. Molecular Dynamics Simulations of the Role of Salinity and Temperature on the Hydrocarbon/Water Interfacial Tension. *Theor. Chem. Acc.* **2017**, *136*, 1−6.
(43) AlRassas, A. M.; Ren, S.; Sun, R.; Thanh, H. V.; Guan, Z. CO_2 Storage Capacity Estimation under Geological Uncertainty Using 3-D Geological Modeling of Unconventional Reservoir Rocks in Shahejie Formation, Block Nv32, China. *J. Pet. Explor. Prod.* **2021**, *11*, 2327−2345.
(44) Al-Anssari, S.; Barifcani, A.; Wang, S.; Maxim, L.; Iglauer, S. Wettability Alteration of Oil-Wet Carbonate by Silica Nanofluid. *J. Colloid Interface Sci.* **2016**, *461*, 435−442.
(45) Al-Mudhafar, W. J. Bayesian and LASSO Regressions for Comparative Permeability Modeling of Sandstone Reservoirs. *Nat. Resour. Res.* **2019**, *28*, 47−62.
(46) Madsen, L.; Lind, I.; Madsen, L.; Und, I.; Denmark, T. U.Adsorption of Carboxylic Acids on Reservoir Minerals From Organic and Aqueous Phase. In *SPE*; 1998; pp 47−51.
(47) Nezhad, M. S.; Wood, D. A.; Sadatshojaei, E.; Esmaeilzadeh, F. New Insight to Experimental Study of Ionic Solutions with a Non-Ionic Surfactant on Wettability, Interfacial Tension and Micro-Model Flooding. *Fuel* **2021**, *285*, No. 119126.
(48) Nangia, S.; Garrison, B. J. Reaction Rates and Dissolution Mechanisms of Quartz as a Function of PH. *J. Phys. Chem. A* **2008**, *112*, 2027−2033.
(49) Bickmore, B. R.; Wheeler, J. C.; Bates, B.; Nagy, K. L.; Eggett, D. L. Reaction Pathways for Quartz Dissolution Determined by Statistical and Graphical Analysis of Macroscopic Experimental Data. *Geochim. Cosmochim. Acta* **2008**, *72*, 4521−4536.
(50) Rodrigues, F. A.; Monteiro, P. J. M.; Sposito, G. Alkali-Silica Reaction the Surface Charge Density of Silica and Its Effect on Expansive Pressure. *Cem. Concr. Res.* **1999**, *29*, 527−530.
(51) Ali, A. M.; Yahya, N.; Mijinyawa, A.; Kwaya, M. Y.; Sikiru, S. Molecular Simulation and Microtextural Characterization of Quartz Dissolution in Sodium Hydroxide. *J. Pet. Explor. Prod. Technol.* **2020**, *10*, 2669−2684.
(52) Kobayashi, M.; Skarba, M.; Galletto, P.; Cakara, D.; Borkovec, M. Effects of Heat Treatment on the Aggregation and Charging of Stöber-Type Silica. *J. Colloid Interface Sci.* **2005**, *292*, 139−147.
(53) Zhuravlev, L. T. The Surface Chemistry of Amorphous Silica. *Zhuravlev Model. Colloids Surfaces A Physicochem. Eng. Asp.* **2000**, *173*, 1−38.
(54) Qi, Z.; Wang, Y.; He, H.; Li, D.; Xu, X. Wettability Alteration of the Quartz Surface in the Presence of Metal Cations. *Energy Fuels* **2013**, *27*, 7354−7359.
(55) Buckley, J. S.; Bousseau, C.; Liu, Y. Wetting Alteration by Brine and Crude Oil: From Contact Angles to Cores. *SPE J.* **1996**, *1*, 341−350.
(56) Buckley, J. S.; Takamura, K.; Morrow, N. R.; Buckley, J. S.; Takamura, K.; Morrow, N. R. Influence of Electrical Surface Charges on the Wetting Properties of Crude Oils. In *SPE Reserv. Eng. (Society Pet. Eng.)*; 1989; Vol. *4*.
(57) Jarrahian, K.; Seiedi, O.; Sheykhan, M.; Sefti, M. V.; Ayatollahi, S. Wettability Alteration of Carbonate Rocks by Surfactants: A Mechanistic Study. *Colloids Surfaces A Physicochem. Eng. Asp.* **2012**, *410*, 1−10.
(58) da Costa, A. A.; Jaeger, P.; Santos, J.; Soares, J.; Trivedi, J.; Embiruçu, M.; Meyberg, G.The Influence of Rock Composition and PH on Reservoir Wettability for Low Salinity Water-CO2 EOR Applications in Brazilian Reservoirs. In *Proc. - SPE Annu. Technol. Conf. Exhib. 2019-Septe*; 2019.
(59) Brady, P. V.; Morrow, N. R.; Fogden, A.; Deniz, V.; Loahardjo, N.; Winoto, A. Electrostatics and the Low Salinity Effect in Sandstone Reservoirs. *Energy Fuels* **2015**, *29*, 666−677.
(60) Yang, J.; Dong, Z.; Dong, M.; Yang, Z.; Lin, M.; Zhang, J.; Chen, C. Wettability Alteration during Low-Salinity Waterflooding and the Relevance of Divalent Ions in This Process. *Energy Fuels* **2016**, *30*, 72−79.
(61) Hua, Z.; Li, M.; Ni, X.; Wang, H.; Yang, Z.; Lin, M. Effect of Injection Brine Composition on Wettability and Oil Recovery in Sandstone Reservoirs. *Fuel* **2016**, *182*, 687−695.
(62) Thomas, F.; Dalmazzone, D.; Morris, J. F. Contact Angle Measurements on Cyclopentane Hydrates. *Chem. Eng. Sci.* **2021**, *229*, No. 116022.
(63) Mahani, H.; Berg, S.; Ilic, D.; Bartels, W. B.; Joekar-Niasar, V. Kinetics of Low-Salinity-Flooding Effect. *SPE J.* **2015**, *20*, 8−20.
(64) Huhtamäki, T.; Tian, X.; Korhonen, J. T.; Ras, R. H. A. Surface-Wetting Characterization Using Contact-Angle Measurements. *Nat. Protoc.* **2018**, *13*, 1521−1538.
(65) Sun, Y.; Li, Y.; Dong, X.; Bu, X.; Drelich, J. W. Spreading and Adhesion Forces for Water Droplets on Methylated Glass Surfaces. *Colloids Surfaces A Physicochem. Eng. Asp.* **2020**, *591*, No. 124562.
(66) Starov, V. M.; Kostvintsev, S. R.; Sobolev, V. D.; Velarde, M. G.; Zhdanov, S. A. Spreading of Liquid Drops over Dry Porous Layers: Complete Wetting Case. *J. Colloid Interface Sci.* **2002**, *252*, 397−408.
(67) Hu, H.; Li, X.; Fang, Z.; Wei, N.; Li, Q. Small-Molecule Gas Sorption and Diffusion in Coal: Molecular Simulation. *Energy* **2010**, *35*, 2939−2944.
(68) Mabudi, A.; Noaparast, M.; Gharabaghi, M.; Vasquez, V. R. A Molecular Dynamics Study on the Wettability of Graphene-Based Silicon Dioxide (Glass) Surface. *Colloids Surfaces A Physicochem. Eng. Asp.* **2019**, *569*, 43−51.
(69) Jia, H.; Lian, P.; Leng, X.; Han, Y.; Wang, Q.; Jia, K.; Niu, X.; Guo, M.; Yan, H.; Lv, K. Mechanism Studies on the Application of the Mixed

https://doi.org/10.1021/acsomega.4c00562
ACS Omega 2024, 9, 20277−20292

Cationic/Anionic Surfactant Systems to Enhance Oil Recovery. *Fuel* **2019**, *258*, No. 116156.
(70) Peter, E.; Sun, R.; Ren, S.; Mutahar, A. Investigating the Low Salinity Effect in a Sandstone Reservoir through Electro-Kinetic Potential Analysis. *Chem. Phys.* **2023**, *574*, No. 112028.
(71) Rostami, P.; Mehraban, M. F.; Sharifi, M.; Dejam, M.; Ayatollahi, S. Effect of Water Salinity on Oil/Brine Interfacial Behaviour during Low Salinity Waterflooding: A Mechanistic Study. *Petroleum* **2019**, *5*, 367−374.
(72) Hosseinzade Khanamiri, H.; Nourani, M.; Tichelkamp, T.; Stensen, J.Å.; Øye, G.; Torsæter, O. Low-Salinity-Surfactant Enhanced Oil Recovery (EOR) with a New Surfactant Blend: Effect of Calcium Cations. *Energy Fuels* **2016**, *30*, 984−991.
(73) Tangparitkul, S.; Charpentier, T. V. J.; Pradilla, D.; Harbottle, D. Interfacial and Colloidal Forces Governing Oil Droplet Displacement: Implications for Enhanced Oil Recovery. *Colloids and Interfaces* **2018**, *2* (3), 30.
(74) Perinelli, D. R.; Cespi, M.; Lorusso, N.; Palmieri, G. F.; Bonacucina, G.; Blasi, P. Surfactant Self-Assembling and Critical Micelle Concentration: One Approach Fits All? *Langmuir* **2020**, *36*, 5745−5753.
(75) Xuefen, Z.; Guiwu, L.; Xiaoming, W.; Hong, Y. Molecular Dynamics Investigation into the Adsorption of Oil-Water-Surfactant Mixture on Quartz. *Appl. Surf. Sci.* **2009**, *255*, 6493−6498.
(76) Liu, J.; Yu, B.; Hong, Q. Molecular Dynamics Simulation of Distribution and Adhesion of Asphalt Components on Steel Slag. *Constr. Build. Mater.* **2020**, *255*, No. 119332.
(77) Gao, Y.; Zhang, Y.; Gu, F.; Xu, T.; Wang, H. Impact of Minerals and Water on Bitumen-Mineral Adhesion and Debonding Behaviours Using Molecular Dynamics Simulations. *Constr. Build. Mater.* **2018**, *171*, 214−222.
(78) Koretsky, C. M.; Sverjensky, D. A.; Sahai, N. A Model of Surface Site Types on Oxide and Silicate Minerals Based on Crystal Chemistry: Implications for Site Types and Densities, Multi-Site Adsorption, Surface Infrared Spectroscopy, and Dissolution Kinetics. *Am. J. Sci.* **1998**, *298*, 349−438.
(79) Chang, Y.; Xiao, S.; Ma, R.; Wang, X.; Zhang, Z.; He, J. Displacement Dynamics of Trapped Oil in Rough Channels Driven by Nanofluids. *Fuel* **2022**, *314*, No. 122760.
(80) Wei, B.; Ning, J.; He, J.; Lu, L.; Wang, Y.; Sun, L. Relation between Brine-Crude Oil-Quartz Contact Angle Formed on Flat Quartz Slides and in Capillaries with Brine Composition: Implications for Low-Salinity Waterflooding. *Colloids Surfaces A Physicochem. Eng. Asp.* **2018**, *555*, 660−667.
(81) Li, S.; Liu, Y.; Xue, L.; Yang, L.; Yuan, Z. A Molecular Insight into the Effect of Key Ions on the Detachment of Crude Oil from Calcite Surface: Implication for Low Salinity Water Flooding in Carbonate Reservoirs. *J. Pet. Sci. Eng.* **2022**, *208*, No. 109562.
(82) Kakati, A.; Sangwai, J. S. Effect of Monovalent and Divalent Salts on the Interfacial Tension of Pure Hydrocarbon-Brine Systems Relevant for Low Salinity Water Flooding. *J. Pet. Sci. Eng.* **2017**, *157*, 1106−1114.
(83) Alvarado, V.; Bidhendi, M. M.; Garcia-Olvera, G.; Morin, B.; Oakey, J. S.Interfacial Visco-Elasticity of Crude Oil - Brine: An Alternative EOR Mechanism in Smart Waterflooding. In *Proc. - SPE Symp. Improv. Oil Recovery*; 2014; Vol. 3, pp 1392−1408.
(84) Al-Otaibi, A. An Investigation into the Roles of Chlorides and Sulphate Salts on the Performance of Low-Salinity Injection in Sandstone Reservoirs: Experimental Approach. *J. Pet. Explor. Prod. Technol.* **2020**, *10*, 2857−2871.
(85) Kumar, S.; Mandal, A. Studies on Interfacial Behavior and Wettability Change Phenomena by Ionic and Nonionic Surfactants in Presence of Alkalis and Salt for Enhanced Oil Recovery. *Appl. Surf. Sci.* **2016**, *372*, 42−51.
(86) Mahmoudvand, M.; Javadi, A.; Pourafshary, P.; Vatanparast, H.; Bahramian, A. Effects of Cation Salinity on the Dynamic Interfacial Tension and Viscoelasticity of a Water-Oil System. *J. Pet. Sci. Eng.* **2021**, *206*, No. 108970.
(87) Wei, B.; Wu, R.; Lu, L.; Ning, X.; Xu, X.; Wood, C.; Yang, Y. Influence of Individual Ions on Oil/Brine/Rock Interfacial Interactions and Oil-Water Flow Behaviors in Porous Media. *Energy Fuels* **2017**, *31*, 12035−12045.
(88) Nasralla, R. A.; Nasr-El-Din, H. A.Impact of Electrical Surface Charges and Cation Exchange on Oil Recovery by Low Salinity Water. In *Soc. Pet. Eng. - SPE Asia Pacific Oil Gas Conf. Exhib. 2011*; 2011; Vol. 2, pp 1714−1731.
(89) Skelton, A. A.; Fenter, P.; Kubicki, J. D.; Wesolowski, D. J.; Cummings, P. T. Simulations of the Quartz$(10\bar{1}1)$/Water Interface: A Comparison of Classical Force Fields, Ab Initio Molecular Dynamics, and x-Ray Reflectivity Experiments. *J. Phys. Chem. C* **2011**, *115*, 2076−2088.
(90) Zhao, J.; Yao, G.; Ramisetti, S. B.; Hammond, R. B.; Wen, D. Molecular Dynamics Simulation of the Salinity Effect on the N-Decane/Water/Vapor Interfacial Equilibrium. *Energy Fuels* **2018**, *32*, 11080−11092.
(91) Koleini, M. M.; Badizad, M. H.; Mahani, H.; Dastjerdi, A. M.; Ayatollahi, S.; Ghazanfari, M. H. Atomistic Insight into Salinity Dependent Preferential Binding of Polar Aromatics to Calcite/Brine Interface: Implications to Low Salinity Waterflooding. *Sci. Rep.* **2021**, *11*, 1−18.
(92) Rücker, M.; Bartels, W. B.; Garfi, G.; Shams, M.; Bultreys, T.; Boone, M.; Pieterse, S.; Maitland, G. C.; Krevor, S.; Cnudde, V.; et al. Relationship between Wetting and Capillary Pressure in a Crude Oil/Brine/Rock System: From Nano-Scale to Core-Scale. *J. Colloid Interface Sci.* **2020**, *562*, 159−169.
(93) Xie, Q.; Saeedi, A.; Pooryousefy, E.; Liu, Y. Extended DLVO-Based Estimates of Surface Force in Low Salinity Water Flooding. *J. Mol. Liq.* **2016**, *221*, 658−665.
(94) Nourani, M.; Tichelkamp, T.; Hosseinzade Khanamiri, H.; Johansen, T.; Karlsen Hov, I.; Gaweł, B.; Torsæter, O.; Øye, G. McGuir Injection and Surfactant Flooding on Silica Surface. *SN Appl. Sci.* **2020**, *2*, 1−13.
(95) Ding, H.; Rahman, S. Experimental and Theoretical Study of Wettability Alteration during Low Salinity Water Flooding-an State of the Art Review. *Colloids Surfaces A Physicochem. Eng. Asp.* **2017**, *520*, 622−639.

https://doi.org/10.1021/acsomega.4c00562
ACS Omega 2024, 9, 20277−20292